DALTON
FULL PAPER

Syntheses, molecular structures and optical nonlinearities of heteroselenometallic W–Se–Pd compounds containing bidentate phosphine ligands

Qian-Feng Zhang,[a,b] Yinling Song,[c] Wai-Yeung Wong,[d] Wa-Hung Leung *[b] and Xinquan Xin *[a]

[a] *Coordination Chemistry Institute and Department of Chemistry, Nanjing University, Nanjing 210093, P. R. China. E-mail: xxin@netra.nju.edu.cn*
[b] *Department of Chemistry, The Hong Kong University of Science and Technology, Clear Water Bay, Kowloon, Hong Kong, P. R. China. E-mail: chleung@ust.hk*
[c] *Department of Physics, Harbin Institute of Technology, Harbin 150001, P. R. China*
[d] *Department of Chemistry, Hong Kong Baptist University, Waterloo Road, Kowloon Tong, Kowloon, Hong Kong, P. R. China*

Received 19th November 2001, Accepted 26th February 2002
First published as an Advance Article on the web 11th April 2002

Reaction of $[NEt_4]_2[WSe_4]$ with $[Pd_2(dppm)_2Cl_2]$ afforded the hexanuclear windmill-shaped compound $[(WSe_4)_2Pd_4(dppm)_2]$ (**1**) {dppm = bis(diphenylphosphino)methane}. Treatment of $[NEt_4]_2[WSe_4]$ with [Pd(P^P)Cl$_2$] gave the dinuclear compounds [(WSe$_4$)Pd(P^P)] {P^P = dppe, 1,2-bis(diphenylphosphino)ethane (**2**); dppp, 1,3-bis(disphenylphosphino)propane (**3**)}. The crystal structures of these heteroselenometallic W–Se–Pd compounds have been determined and their nonlinear optical properties were studied with an 8 ns pulsed laser at 532 nm. It was found that compounds **1**–**3** show predominantly nonlinear refraction and negligible nonlinear absorption. Compound **1** exhibits a considerable self-defocusing properties with the nonlinear refractivity (n_2) value estimated to be -3.74×10^{-10} cm^2 W^{-1} M^{-1}. The optical limiting thresholds of compounds **1**, **2** and **3** were determined to be *ca.* 3.1, 6.5 and 7.2 J cm^{-2}, respectively.

Introduction

The tetrathiometallates $[MS_4]^{2-}$ (M = Mo, W) exhibit rich structural chemistry upon coordination to inorganic and organometallic fragments.[1] The resulting heterometallic complexes possess more or less extended structures, and often show interesting electronic and optical properties.[2] For example, strong third-order nonlinear optical (NLO) properties were observed for certain heterometallic Mo(W)/Cu(Ag,Au)/S clusters.[2,3] In order to elucidate the structure–property relationship for this new class of NLO materials, a large number of heterometallic clusters based on tetrathiometallates have been synthesized recently. Whereas an extension of the cluster chemistry of the analogous tetraselenometallates $[MSe_4]^{2-}$ (M = Mo or W) has been realized only very recently, the study of the NLO properties of heteroselonemetallic compounds is very limited to date.[4]

In our search for new NLO materials based on inorganic clusters, we have gradually shifted our attention from heterothiometallic to heteroselenometallic clusters, in the belief that the heavy atom effect may result in an improvement in the NLO properties of the metal clusters.[5,6] Additionally, selenium-containing compounds may also find applications as precursors for low bandgap semiconductors.[7] Recently, we have studied the reactions of $[MSe_4]^{2-}$ (M = Mo or W) with d^{10} metal ions, namely Cu^I, Ag^I and Au^I, and investigated the NLO properties of the resulting heteroselenometallic clusters.[5,8] In continuation of our efforts to understand the structure–property relationship for inorganic NLO materials, we extend our study to heteroselenometallic clusters derived from metal ions with partially filled d shell configurations, which are expected to possess rich structural chemistry. We herein report the syntheses, molecular structures and NLO properties of heteroselenometallic W–Se–Pd compounds $[(WSe_4)_2Pd_4(dppm)_2]$ (**1**) {dppm = bis(diphenylphosphino)methane}, [(WSe$_4$)Pd(dppe)] (**2**) {dppe = 1,2-bis(diphenylphosphino)ethane} and [(WSe$_4$)Pd(dppp)] (**3**) {dppp = 1,3-bis(diphenylphosphino)propane}. We have communicated preliminary results on the structural study of **1** previously.[9]

Experimental

All syntheses were performed in oven-dried glassware under a purified nitrogen atmosphere using standard Schlenk techniques. The solvents were purified by conventional methods and degassed prior to use. The ligands dppm, dppe and dppp, and [PdCl$_2$] were purchased from Aldrich and were used without further purification. The compound $[NEt_4]_2[WSe_4]$ was prepared by an improvement version of the literature method.[10] The compounds $[Pd_2(dppm)_2Cl_2]$ [11] and [Pd(cod)Cl$_2$] (cod = 1,5-cyclooctadiene) [12] were synthesized according to the literature methods.

Preparations

$[(WSe_4)_2Pd_4(dppm)_2]\cdot 2dmf$ ($1\cdot 2dmf$). To a solution of $[NEt_4]_2[WSe_4]$ (0.38 g, 0.50 mmol) in *N*,*N*-dimethylformamide (dmf) (10 ml) was slowly added a solution of $[Pd_2(dppm)_2Cl_2]$ (0.55 g, 0.50 mmol) in CH$_2$Cl$_2$ (20 cm^3) at room temperature. The deep red solution gradually changed to brown. The mixture was stirred for 1 h and then filtered to afford a dark red filtrate. Et$_2$O was diffused into the filtrate for one day, resulting in the formation of black crystals suitable for a single-crystal X-ray diffraction study, which were identified as **1**·2dmf. Yield: 0.36 g (42%). NMR (CDCl$_3$): ^{1}H, δ 5.47 (4H, CH$_2$), 6.80–7.64 (40H, Ph), 2.91 (12H, *Me*$_2$NCHO), 8.12 (2H, CHO); ^{31}P{^{1}H}, δ 1.47(s). IR (KBr pellets, cm^{-1}): [ν(C=O)] 1668.3 (s), [ν(P–C)] 530.3 (s), 509.1 (s), 478.3 (s), 443.5 (s); [ν(W=Se)] 314.2

Table 1 Crystallographic data for compounds **1**·2dmf, **2** and **3**·CH_2Cl_2

	1·2dmf	**2**	**3**·CH_2Cl_2
Empirical formula	$C_{50}H_{44}P_4Se_8Pd_4W_2$·2dmf	$C_{26}H_{24}P_2Se_4PdW$	$C_{27}H_{26}P_2Se_4PdW·CH_2Cl_2$
Formula weight	2340.04	1004.48	1103.43
Crystal system	Monoclinic	Triclinic	Monoclinic
Space group	$P2_1/c$	$P\bar{1}$	$P2_1/m$
a/Å	10.5525(1)	9.3350(5)	10.0512(6)
b/Å	15.1794(2)	10.6129(6)	14.8092(9)
c/Å	21.2565(2)	15.6580(9)	10.8528(7)
α/°		82.728(1)	
β/°	98.726(1)	76.978(1)	91.481(1)
γ/°		79.735(1)	
U/Å^3	3365.47(6)	1481.1(1)	1614.9(2)
Z	2	2	2
T/K	293	293	293
μ(Mo-Kα)/mm^{-1}	8.911	9.542	8.906
Reflections collected	8263	8583	7972
Trans. factor range	0.242–0.524	0.692–0.989	0.394–0.995
Unique reflections/R(int)	4569/0.0933	6279/0.0208	2949/0.0472
$R1$, $wR2$ [$I > 2\sigma(I)$]	0.0534, 0.1029	0.0364, 0.1002	0.0534, 0.1517
$R1$, $wR2$ [all data]	0.1252, 0.1261	0.0414, 0.1045	0.0563, 0.1549

(s), [ν(W–Se)] 297.3 (m), 291.5 (w). MS (FAB): m/z 2194 ($M^+ - 2dmf + 1$), 1425 ($M^+ - 2dmf - 2dppm + 1$). Found: C, 29.28; H, 2.19; N, 1.16; calc. for $C_{50}H_{44}P_4Se_8Pd_4W_2$·2dmf: C, 28.74; H, 2.50; N, 1.20%.

[(WSe_4)Pd(dppe)] (2). To a slurry of [Pd(cod)Cl_2] (0.14 g, 0.50 mmol) and dppe (0.26 g, 0.65 mmol) in CH_2Cl_2 (15 cm^3) was added a solution of [NEt_4]$_2$[WSe_4] (0.38 g, 0.50 mmol) in MeCN (10 cm^3). The mixture was stirred at room temperature for 30 min, during which time the mixture acquired an orange color. The solution was separated from a small amount of red precipitate by filtration. The resulting filtrate was diffused with diethyl ether vapor and orange prism-shaped crystals of **2** were obtained after one day. Yield: 0.42 g (68%). NMR [$(CD_3)_2SO$]: ^{1}H, δ 3.11 (d, 4H, CH_2), 7.69–7.75 (20H, Ph); ^{31}P{^{1}H}, δ 58.54(s). IR (KBr pellets, cm^{-1}): [ν(P–C)] 531.5(s), 511.6(s), 448.4(s); [ν(W=Se)] 313.5 (s), [ν(W–Se)] 295.4 (m). MS (FAB): m/z 1005 ($M^+ + 1$), 607 ($M^+ -$ dppe $+ 1$). Found: C, 31.01; H, 2.38; calc. for $C_{26}H_{24}P_2Se_4PdW$: C, 31.09; H, 2.41%.

[(WSe_4)Pd(dppp)]·CH_2Cl_2 (3·CH_2Cl_2). The preparation was similar to that of **2**, using dppp (0.21 g, 0.50 mmol) instead of dppe. Yield: 0.0.39 g (62%). NMR [$(CD_3)_2SO$]: ^{1}H, δ 1.26 (2H, $CH_2CH_2CH_2$), 2.18 (4H, PCH_2), 7.46–7.91 (20H, Ph); ^{31}P{^{1}H}, δ 32.95(s). IR (KBr pellets, cm^{-1}): [ν(P–C)] 530.8(s), 512.4(s), 449.7(s); [ν(W=Se)] 312.7 (s), [ν(W–Se)] 296.2 (m). MS (FAB): m/z 1019 ($M^+ + 1$), 607 ($M^+ -$ dppp $+ 1$). Found: C, 30.76; H, 2.48; calc. for $C_{27}H_{26}P_2Se_4PdW·CH_2Cl_2$: C, 30.48; H, 2.56%.

X-Ray crystallography

Well-developed single-crystals of **1**·2dmf (0.46 × 0.12 × 0.08 mm), **2** (0.32 × 0.20 × 0.16 mm) and **3**·CH_2Cl_2 (0.35 × 0.23 × 0.18 mm) were mounted on glass fibers. Diffraction data were collected on a Siemens SMART CCD area-detector diffractometer equipped with graphite-monochromated Mo-Kα radiation (λ = 0.71073 Å) by using an ω scan technique (for **1**·2dmf, $1.66 < \theta < 28.30°$; for **2**, $1.96 < \theta < 27.50°$; for **3**·CH_2Cl_2, $1.88 < \theta < 25.00°$). The collected frames were processed with the software SAINT.[13] The data were corrected for absorption using the program SADABS.[14] Structures were solved by direct methods and refined by full-matrix least-squares on F^2 using the SHELXTL software package.[15] All non-hydrogen atoms were refined anisotropically. The positions of all hydrogen atoms were generated geometrically (C–H bond fixed at 0.96 Å), assigned isotropic thermal parameters and allowed to ride on their respective parent C atoms before the final cycle of least-squares refinement. The largest peaks in the final difference maps had heights of 2.393 (for **1**·2dmf), 1.696 (for **2**) and 3.892 e Å^{-3} (for **3**·CH_2Cl_2) and are in the vicinity of the W atoms. Crystallographic data are summarized in Table 1.

CCDC reference numbers 132668, 174697 and 174698.

See http://www.rsc.org/suppdata/dt/b1/b110583n/ for crystallographic data in CIF or other electronic format.

Spectroscopic, NLO and other measurements

Electronic absorption spectra were obtained in dmf solutions on a Shimazu UV-3000 spectrophotometer. Infrared spectra were recorded on a Nicolet 170sx FT–IR spectrophotometer. NMR spectra (in KBr pellets) were recorded on a Bruker DPX-300 Fourier-transform spectrometer. Chemical shifts (δ, ppm) were reported with reference to $SiMe_4$ (^{1}H) and H_3PO_4 (^{31}P). Mass spectra were obtained on a Finnigan TSQ-7000 spectrometer. Elemental analyses were performed by Medac Ltd., Surrey, UK.

A dmf solution of the clusters **1**, **2** or **3** was placed in a 5 mm quartz cuvette for optical limiting property measurements, which were performed with linearly polarized 8 ns pulses at 532 nm generated from a Q-switched frequency-doubled Nd : YAG laser. The cluster is stable toward air and laser light under experimental conditions. The spatial profiles of the pulsed laser were focused on the sample cell with a 15 cm focal length mirror. The spot radius of the laser beam was measured to be 55 µm (half-width at $1/e^2$ maximum). The energies of the input and output pulses were measured simultaneously by precision laser detectors (Rjp-735 energy probes) while the incident energy was varied using a Newport Com. Attenuator. The interval between the laser pulses was chosen as 1 s to avoid influences from thermal and long-term effects.

The effective third-order NLO absorptive and refractive properties of cluster **1** were recorded by moving the sample along the axis of the incident laser beam (z direction), with respect to the focal point, instead of being positioned at its focal point, and an identical set-up was adopted in the experiments to measure the z-scan data. An aperture of 0.5 mm radius was placed in front of the detector to assist in the measurement of the nonlinear optical absorption and self-focusing effect.

Results and discussion

Synthesis and spectroscopy

Treatment of [$Pd_2(dppm)_2Cl_2$] with [NEt_4]$_2$[WSe_4] in CH_2Cl_2–dmf afforded the neutral hexanuclear cluster [$(WSe_4)_2Pd_4(dppm)_2$]·2dmf (**1**·2dmf). For the formation of **1**, it seems that the displacement of two chlorides and one dppm ligand in $[Pd_2(dppm)_2Cl_2]$ to give an unsaturated intermediate $[Pd_2(dppm)]^{2+}$ that coordinated to $[WSe_4]^{2-}$ was involved. It may be noted that similar hexanuclear clusters have also been isolated from the reaction of $[MS_4]^{2-}$ (M = Mo or W) with the Pd^{II} starting material $[Pd(dppm)Cl_2]$.[16] On the other hand, treatment of $[PdCl_2(P^\wedge P)]$ with $[NEt_4]_2[WSe_4]$ afforded the dinuclear compounds $[(WSe_4)Pd(P^\wedge P)]$ {$P^\wedge P$ = dppe (**2**), dppp (**3**)}. Thus, it appears that, in the present system, the use of dppm as an ancillary ligand facilitates the formation of the hexanuclear heterometallic clusters. dppm is a common bridging ligand for constructing binuclear metal complexes with novel chemical properties. The flexibility of the methylene bridge in dppm allows the metal–metal separations in dinuclear *trans*-bridged complexes to vary from 2.1 to 3.5 Å.[17] Thus, with dppm, hexanuclear heterometallic clusters with Pd–Pd bonds were isolated in the present system. By contrast, dppe and dppp usually act as bidentate ligands that bind to metal ions to form stable five- or six-membered metallocycle.[18] Therefore, it is not surprising that dinuclear complexes **2** and **3** were obtained upon coordination of $[WSe_4]^{2-}$ to $[Pd(P^\wedge P)]^{2+}$ ($P^\wedge P$ = dppe or dppp).

The IR spectra of compounds **1**–**3** display typical absorption peaks at about 1475, 1434, 995, 690, 530, 510 and 450 cm^{-1}, which are characteristic for bidentate dppm, dppe and dppp ligands. The W–Se stretching vibrations for **1**–**3** were observed in the expected lower wavenumber region of 290–315 cm^{-1}. The W–Se(terminal) absorptions were found at 312–314 cm^{-1}, which are obviously blue-shifted compared to the W–Se(bridging) absorptions at about 296 cm^{-1}. This is also consistent with the difference in W–Se bond length in the solid state structures [W–Se(terminal) 2.2650(13)–2.2719(7) Å *cf.* W–Se(bridging) 2.3382(10)–2.4149(10) Å] (see later section). The ^{31}P NMR spectra of compounds **1**–**3** show single resonances due to the magnetically equivalent phosphorus nuclei in these compounds. The ^{31}P resonances for compounds **1**–**3** are more downfield than those for the corresponding $Pd(P^\wedge P)$ starting materials, suggesting that the Pd–Se interactions result in charge transfer from P to Pd.[19] This is probably a reflection of better orbital overlap between Pd and soft Se than that between Pd and harder Cl. The FAB^+ mass spectra of compounds **1**–**3** exhibit molecular ions corresponding to ($M^+ + 1$) and ($M^+ - P^\wedge P$) with the characteristic isotopic distribution patterns.

Crystal structures

The molecular structure of centrosymmertric $[(WSe_4)_2Pd_4(dppm)_2]$, shown in Fig. 1, comprises two $[Pd_2(dppm)]^{2+}$ fragments bridged by two $[WSe_4]^{2-}$ moieties. Each $[WSe_4]^{2-}$ tetrahedron binds to two Pd^I centres across its two edges, leaving a terminal W=Se bond. The coordination environment of each Pd is the same, that is, each is asymmetrically surrounded by one μ_3-Se, one μ-Se, one Pd and one P, resulting in a highly distorted square-planar arrangement. The dppm-bridged Pd–Pd bond in **1** [2.6346(10) Å] is similar to that in $[Pd_2(\mu\text{-dppm})_2Cl_2]$ [2.699(5) Å].[20] This indicates that structure of cluster **1** is still of the A-frame type, which is well documented for dinuclear Pd^I compounds.[21] The average Pd–μ_3–Se bond length in **1** of 2.4660(11) Å is slightly shorter than the average Pd–μ–Se bond length of 2.4817(12) Å, suggesting that the d–p hybridization between Pd and μ_3-Se atoms is stronger than that between Pd and μ-Se atoms.[9] Another structural feature of cluster **1** is an almost co-planar arrangement of eight atoms, Se(2), Se(3), Pd(1) and Pd(2), and their symmetry equivalents Se(2A), Se(3A), Pd(1A) and Pd(2A), with a maximum derivation of 0.06 Å. The coordination geometry of the W centers remains nearly tetrahedral, with the bond angles ranging from 107.71(4) to 110.66(5)°. The W–Se bond lengths fall into three categories: the W–Se_t, W–μ–Se and W–μ_3–Se bond distances are 2.2699(14), 2.3398(11) and 2.4149(10) Å, respectively. The average W ··· Pd separation of 2.9439(8) Å for **1** is comparable to those reported for related W–S–Pd complexes[18,22,23] and the Pd^{II} compounds **2** and **3** (see Table 2).

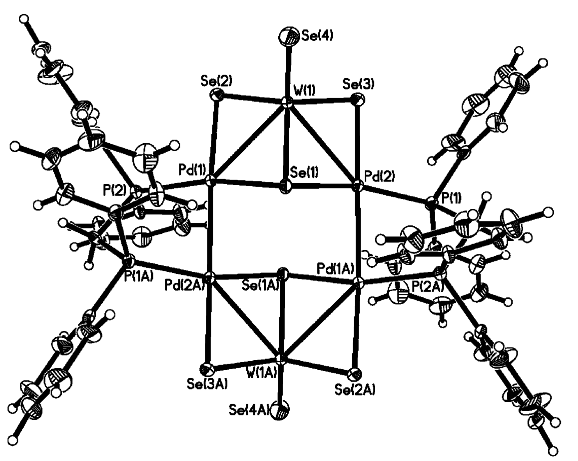

Fig. 1 Crystal structure of $[(WSe_4)_2Pd_4(dppm)_2]$ (**1**), showing 30% thermal probability ellipsoids.

The solid state structures of compounds **2** and **3** shown in Fig. 2 and 3, respectively. In these structures, the $[WSe_4]^{2-}$ tetra-

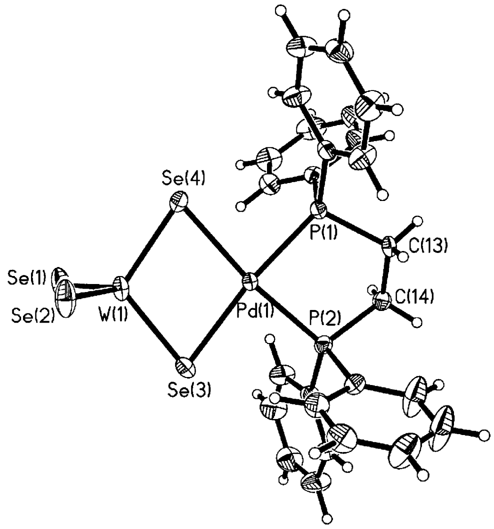

Fig. 2 Crystal structure of $[(WSe_4)Pd(dppe)]$ (**2**), showing 25% thermal probability ellipsoids.

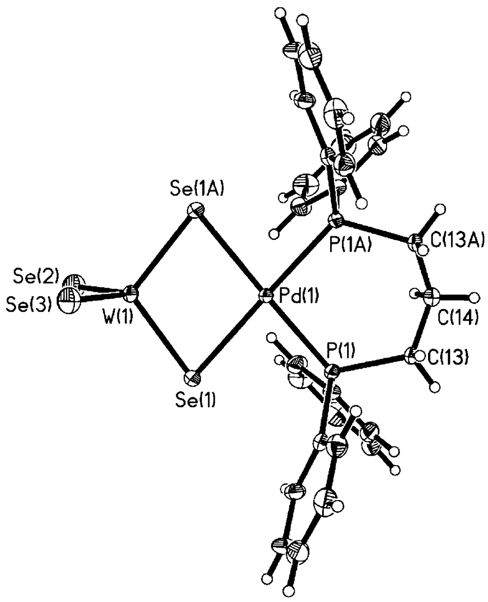

Fig. 3 Crystal structure of $[(WSe_4)Pd(dppp)]$ (**3**), showing 25% thermal probability ellipsoids.

Table 2 Comparison of selected bond parameters for **1**–**3** and related W–S(Se)–Pd compounds[a]

Compound	W–S$_t$(Se$_t$)[b]	W–S$_b$(Se$_b$)[b]	Pd–S(Se)	W · · · Pd	S(Se)–W–S(Se)	S(Se)–Pd–S(Se)	Ref.
[(WS$_4$)Pd(dppe)]	2.135(7)–2.147(8) av. 2.141(7)	2.228(6)–2.236(5) av. 2.232(5)	2.351(6)–2.354(5) av. 2.353(5)	2.887(2)	105.7(3)–110.5(3) av. 109.5(3)	98.3(3)	18(*a*)
[(WS$_4$)Pd(dppp)]	2.137(2)–2.163(2) av. 2.150(2)	2.217(2)–2.230(2) av. 2.224(2)	2.360(2)–2.368(2) av. 2.364(2)	2.9259(6)	104.88(8)–110.74(7) av. 109.46(8)	96.43(7)	18(*b*)
[(WS$_4$)$_2$Pd$_4$(dppm)$_2$]	2.133(2)	2.203(2)–2.274(2) av. 2.230(2)	2.348(2)–2.376(2) av. 2.364(2)	2.8689(6)	106.54(7)–111.66(9) av. 109.46(8)	98.64(7)–99.27(7) av. 98.96(7)	16
[NEt$_4$][(WS$_4$)Pd(S$_2$CNC$_4$H$_8$)]	2.148(2)–2.153(2) av. 2.150(2)	2.235(2)	2.336(2)–2.342(2) av. 2.339(2)	2.8669(7)	105.51(7)–111.37(9) av. 109.47(9)	99.10(8)	23
[NEt$_4$]$_2$[(WS$_4$)$_2$Pd]	2.148(3)	2.238(3)–2.240(3) av. 2.239(3)	2.347(3)–2.359(3) av. 2.353(3)	2.9008(5)	105.2(1)–111.5(1) av. 109.5(1)	81.8(1)–98.2(1) av. 90.0(1)	23
[Ni(bpy)$_3$][(WS$_4$)$_2$Pd][c]	2.135(5)–2.157(5) av. 2.148(5)	2.225(4)–2.239(4) av. 2.234(4)	2.341(4)–2.352(4) av. 2.346(4)	2.897(1)–2.900(1) av. 2.898(1)	104.7(1)–112.0(2) av. 109.4(2)	81.8(1)–98.2(1) av. 90.3(1)	22
1·2dmf	2.2699(14)	2.338(1)–2.415(1) av. 2.365(1)	2.465(1)–2.490(1) av. 2.474(1)	2.938(1)–2.950(1) av. 2.944(1)	107.71(4)–110.25(5) av. 108.88(4)	102.13(4)–102.35(4) av. 102.24(4)	This work
2	2.269(1)–2.273(1) av. 2.271(1)	2.353(1)–2.361(1) av. 2.357(1)	2.460(1)–2.462(1) av. 2.462(1)	2.9628(4)	107.30(2)–110.74(3) av. 109.47(4)	100.98(2)	This work
3·CH$_2$Cl$_2$	2.265(1)–2.267(1) av. 2.266(1)	2.349(1)	2.477(1)	3.0302(8)	106.05(4)–110.49(3) av. 109.47(3)	98.49(4)	This work

[a] Bond distances in Å and bond angles in °, with e.s.d.s in parentheses. [b] t = terminal, b = bridging. [c] bpy = 2,2′-bipyridine.

hedron binds to the [Pd(P^P)]$^{2+}$ (P^P = dppe for **2**, dppp for **3**) across one edge, leaving two terminal W=Se bonds. A minor configurational difference between the two compounds is that the dppe ligand in **2** binds to the Pd to form a five-membered ring, while the dppp ligand in **3**·CH$_2$Cl$_2$ binds to the Pd to form a six-membered ring. The structural difference between the two compounds is an approximate two-fold rotation for **2** and an exact mirror plane for **3**·CH$_2$Cl$_2$. The coordination geometry around Pd in these complexes is distorted square planar. The average Pd–Se and Pd–P bond lengths are 2.4609(7) and 2.2793(13) Å, respectively, for **2**, and 2.4773(9) and 2.2982(17) Å, respectively, for **3**·CH$_2$Cl$_2$, which agree well with the average lengths of these bonds in compound **1**. Selected structural parameters for related W–S(Se)–Pd compounds are compiled in Table 2 for comparison.

NLO properties

The nonlinear optical properties of compounds **1**, **2** and **3** were investigated using the *z*-scan technique.[24] Similar to the analogous W–S–Pd complexes,[16,18*b*,23] the NLO properties of compounds **1**, **2** and **3** are relatively simple: they show dominantly nonlinear refraction and their nonlinear absorption is negligible. Fig. 4 depicts typical *z*-scan measurements for a 1.25 × 10^{-3} mol dm^{-3} solution of compound **1** in dmf. The nonlinear refractive components plotted with the filled circles were assessed by dividing the normalised *z*-scan data obtained under the closed aperture configuration by those obtained under the open aperture configuration. The valley and peak occur at about equal distances from the focus. It can be seen that the difference in valley–peak positions ΔZ_{V-P} is 10 mm and the difference between the normalised transmittance values at the valley and peak positions ΔT_{V-P} is 0.04. These results suggest an effectively weak third-order optical nonlinearity.[24] The solid curve is an eye guide for comparison and from which the effective nonlinear refractivity (n_2) value was estimated to be -3.74×10^{-10} cm^2 W^{-1} M^{-1} for **1**. Compound **1** shows a negative n_2 value, indicating that the laser beam propagating in it undergoes a self-defocusing process in the nonlinear

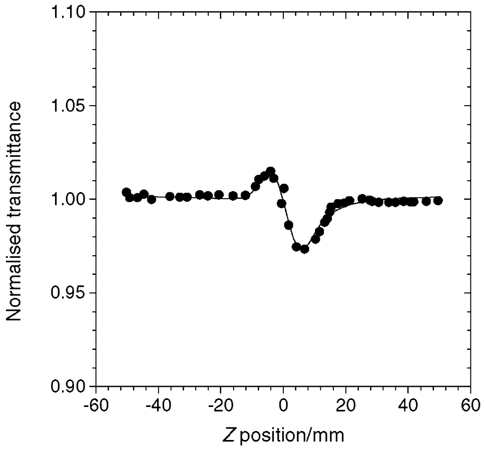

Fig. 4 *z*-Scan data from a 1.25 × 10^{-3} mol dm^{-3} solution of **1** in dmf at 532 nm with incident energy of 180 μJ. The data was collected by moving the sample along the axis of the incident beam (*z*-direction) with respect to the focal point. An aperture of 1 mm radius was placed in front of the detector measuring the self-defocusing effect. The solid curves are the theoretical fit based on eqn. (1) and (2).

$$T(Z) = \frac{1}{\pi^{1/2} q(Z)} \int_{-\infty}^{\infty} \ln[1 + q(z)] e^{-\tau^2} d\tau \qquad (1)$$

$$q(Z) = \alpha_2 I_i(Z) \frac{(1 - e^{-\alpha_0 L})}{\alpha_0} \qquad (2)$$

Table 3 Comparison of NLO parameters for **1**–**3** and related W–S(Se)–Pd compounds[a]

Compound	Structural type	$10^{-3}\alpha_0$/cm^{-1} M^{-1}	α_2/cm W^{-1} M^{-1}	$10^{10}n_2$/cm^2 W^{-1} M^{-1}	Ref.
[(MoS$_4$)Pd(dppp)]	Linear	5.50	2.0×10^{-5}	−1.10	18(*a*)
[(WS$_4$)Pd(dppp)]	Linear	7.57	n.d.[b]	n.d.[b]	18(*a*)
[(WS$_4$)$_2$Pd$_4$(dppm)$_2$]	Windmill	2.10	1.2×10^{-6}	−1.50	16
[NEt$_4$][(WS$_4$)Pd(S$_2$CNC$_4$H$_8$)]	Linear	1.08	—[c]	−0.68	23
[NEt$_4$]$_2$[(WS$_4$)$_2$Pd]	Linear	0.62	3.5×10^{-6}	−0.75	23
1	Windmill	1.94	5.9×10^{-5}	−3.74	This work
2	Linear	2.68	—[c]	−0.96	This work
3	Linear	3.35	—[c]	−1.24	This work

[a] α_0 is the linear absorption coefficient; α_2 is the nonlinear absorption coefficient and n_2 is the nonlinear refractive index. [b] Not determined. [c] Negligible.

refractive effects. Table 3 lists the measured nonlinear absorption coefficient (α_2) and nonlinear refractive index (n_2) for some related heterometallic W–S(Se)–Pd compounds. Comparatively, heteroselenometallic compounds **1**–**3**, together with other sulfur analogues, are inferior in NLO properties to most Mo(W)–S(Se)–Cu(Ag,Au) cluster compounds.[3,8,25] This may be attributed to their structural variations. Univalent coinage metal ions with a closed shell d^{10} configuration, namely Cu$^+$, Ag$^+$ and Au$^+$, are either tetrahedrally or trigonally coordinated, whereas Pd$^+$ and Pd^{2+}, with partially filled d shells, prefer planar coordination geometry. The greater the incorporation of metal ions, the more sublevels can be introduced into the energy hierarchy. Thus, for Mo(W)–S(Se)–Cu(Ag,Au) clusters, more spin-allowed excited state to excited state transitions can take place, and hence larger nonlinear absorption was observed.[23,26]

The optical limiting effects (OL) of compounds **1**–**3** were also investigated. Fig. 5 shows the 8 ns optical limiting experimental results for the samples in dmf solutions at the same concentration (1.25×10^{-3} mol dm^{-3}). Experiments with dmf alone afforded no detectable OL effect. This indicates that the solvent contribution is negligible. The light energy transmitted started to deviate from Beer's law as the input light fluence reached a saturation value, and the sample solution became increasingly less transparent as the fluence rose. Thus, the transmittances of the samples were found to decrease as the laser fluence increases, characteristic of optical limiting.[27] The limiting threshold was defined as the incident fluence at which the transmittance falls to 76% of the linear transmittance. From Fig. 5, the limiting thresholds of compounds **1**, **2** and **3** were determined to be *ca.* 3.1, 6.5 and 7.2 J cm^{-2}, respectively. The saturation fluence transmitted is *ca.* 2 J cm^{-2}. Compared with the low-nuclearity compounds **2** and **3**, polynuclear compound **1** has a relatively large optical limiting capability.

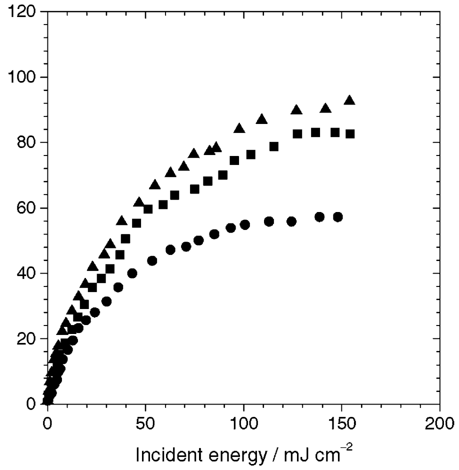

Fig. 5 Optical limiting effect of compounds **1** (filled circle), **2** (filled squares) and **3** (filled triangles) in dmf solutions (1.25×10^{-3} mol dm^{-3}).

In summary, we have synthesised and characterised three heteroselenometallic W–Se–Pd compounds containing bidentate phosphine ligands. The hexanuclear windmill-shaped compound [(WSe$_4$)$_2$Pd$_4$(dppm)$_2$] (**1**) was prepared from the reaction of [NEt$_4$]$_2$[WSe$_4$] with [Pd$_2$(dppm)$_2$Cl$_2$]. On the other hand, reaction of [WSe$_4$]$^{2-}$ with [Pd(P^P)Cl$_2$] (P^P = dppe or dppp) gave the dinuclear compounds [(WSe$_4$)Pd(P^P)]. The nonlinear optical properties of these three heterometallic compounds show predominantly nonlinear refraction and negligible nonlinear absorption. This result suggests that geometry of the coordinated metal in heterometallic cluster compounds with [MQ$_4$]$^{2-}$ (M = Mo or W, Q = S or Se) moiety has an influence on their NLO properties. Efforts are being made to obtain further evidence to support this suggestion.

Acknowledgements

We thank the Ministry of Education of China and the Hong Kong University of Science and Technology for support.

References

1 (*a*) A. Müller, E. Diemann, R. Josters and H. Bögge, *Angew. Chem., Int. Ed. Engl.*, 1981, **20**, 934; (*b*) K. E. Howard, T. B. Rauchfuss and A. L. Rheingold, *J. Am. Chem. Soc.*, 1986, **108**, 297; (*c*) K. E. Howard, T. B. Rauchfuss and S. R. Wilson, *Inorg. Chem.*, 1988, **27**, 3561; (*d*) I. G. Dance and K. Fisher, *Prog. Inorg. Chem.*, 1994, **41**, 637.

2 (*a*) S. Shi, W. Ji, S. H. Tang, J. P. Lang and X. Q. Xin, *J. Am. Chem. Soc.*, 1994, **116**, 3615; (*b*) S. Shi, W. Ji and X. Q. Xin, *J. Phys. Chem.*, 1995, **99**, 894; (*c*) P. E. Hoggard, H. W. Hou, X. Q. Xin and S. Shi, *Chem. Mater.*, 1996, **8**, 2218.

3 (*a*) H. W. Hou, X. Q. Xin and S. Shi, *Coord. Chem. Rev.*, 1996, **153**, 25; (*b*) S. Shi, Z. Lin, Y. Mo and X. Q. Xin, *J. Phys. Chem.*, 1996, **100**, 10696.

4 (*a*) L. C. Roof and J. W. Kolis, *Chem. Rev.*, 1993, **93**, 1037; (*b*) R. J. Salm and J. A. Ibers, *Inorg. Chem.*, 1994, **33**, 4216; (*c*) R. J. Salm, A. Misetic and J. A. Ibers, *Inorg. Chim. Acta*, 1995, **240**, 239; (*d*) M. C. Hong, Q. F. Zhang, R. Cao, D. X. Wu, J. T. Chen, W. J. Zhang, H. Q. Liu and J. X. Lu, *Inorg. Chem.*, 1997, **36**, 6251.

5 (*a*) Q. F. Zhang, Y. N. Xiong, T. S. Lai, W. Ji and X. Q. Xin, *J. Phys. Chem. B*, 2000, **104**, 3446; (*b*) Y. L. Song, S. L. Qu, Y. X. Wang, Q. F. Zhang and X. Q. Xin, *Chem. Phys. Lett.*, 2001, **338**, 108.

6 (*a*) A. Dogariu, T. Xia, D. J. Hagan, A. A. Said, E. W. Van Stryland and N. Bloembergen, *J. Opt. Soc. Am. B*, 1996, **14**, 796; (*b*) P. Ge, S. H. Tang, W. Ji, S. Shi, H. W. Hou, D. L. Long, X. Q. Xin, S. F. Lu and Q. J. Wu, *J. Phys. Chem. B*, 1997, **101**, 27.

7 See any issue of *"The Bulletin of the Selenium-Tellurium Development Association"*, Grimbergen, Belgium.

8 (*a*) Q. F. Zhang, S. S. S. Raj, H. K. Fun and X. Q. Xin, *Chem. Lett.*, 1999, 619; (*b*) Q. F. Zhang, W. H. Leung, X. Q. Xin and H. K. Fun, *Inorg. Chem.*, 2000, **39**, 417; (*c*) Q. F. Zhang, M. T. Bao, M. C. Hong, R. Cao, Y. L. Song and X. Q. Xin, *J. Chem. Soc., Dalton Trans.*, 2000, 605; (*d*) Q. F. Zhang, W. H. Leung, Y. L. Song, M. C. Hong, C. H. L. Kennard and X. Q. Xin, *New J. Chem.*, 2001, **25**, 465.

9 Q. F. Zhang, S. S. S. Raj, M. C. Hong, R. Cao, H. K. Fun and X. Q. Xin, *Inorg. Chem. Commun.*, 1999, **2**, 272.

10 S. C. O'Neal and J. W. Kolis, *J. Am. Chem. Soc.*, 1988, **110**, 1971.

11 A. L. Balch and L. S. Benner, *Inorg. Synth.*, 1990, **28**, 340.

12 D. Drew and J. R. Doyle, *Inorg. Synth.*, 1990, **28**, 346.

13 SAINT Reference Manual, Siemens Energy and Automation, Madison, WI, USA, 1994–1996.

14 G. M. Sheldrick, SADABS, Program for Absorption Correction Using Area Detector Data, University of Göttingen: Göttingen, Germany, 1996.

15 G. M. Sheldrick, SHELXTL, version 5.1, Reference Manual, Siemens Energy and Automation, Madison, WI, USA, 1997.

16 H. Zheng, W. H. Leung, W. Tan, D. Long, W. Ji, J. Chen, F. Xin and X. Xin, *J. Chem. Soc., Dalton Trans.*, 2000, 2145.

17 M. M. Olmstead, C. H. Lindsay, L. S. Benner and A. L. Balch, *J. Organomet. Chem.*, 1979, **179**, 289.

18 (*a*) B. Wu, W. Zhang, X. Huang, X. Wu and S. Yu, *Polyhedron*, 1997, **16**, 801; (*b*) H. G. Zheng, W. L. Tan, G. C. Jin, W. Ji, Q. H. Jin, X. Y. Huang and X. Q. Xin, *Inorg. Chim. Acta*, 2000, **305**, 14.

19 R. W. M. Wardle, C. H. Mahler, C.-N. Chau and J. A. Ibers, *Inorg. Chem.*, 1988, **27**, 2790.

20 R. G. Holloway, B. R. Penfold, R. Colton and M. J. McCormick, *J. Chem. Soc., Chem. Commun.*, 1976, 485.

21 P. Braunstein, J. Kervennal and J.-L. Richert, *Angew. Chem., Int. Ed. Engl.*, 1985, **24**, 768.

22 C. Potvin, J.-M. Manoli and F. Séchersse, *Inorg. Chim. Acta*, 1990, **168**, 173.

23 D. L. Long, W. T. Wong, S. Shi, X. Q. Xin and J. S. Huang, *J. Chem. Soc., Dalton Trans.*, 1997, 4361.

24 (*a*) M. Sheik-Bahae, A. A. Said and E. W. Van Stryland, *Opt. Lett.*, 1989, **14**, 955; (*b*) M. Sheik-Bahae, A. A. Said, T. H. Wei, D. J. Hagan and E. W. Van Stryland, *IEEE J. Quantum Electron*, 1990, **26**, 760.

25 (*a*) D. L. Long, S. Shi, X. Q. Xin, B. S. Lou, L. R. Chen, X. Y. Huang and B. S. Kang, *J. Chem. Soc., Dalton Trans.*, 1996, 2617; (*b*) H. Zheng, W. Ji, M. L. K. Low, G. Sakane, T. Shibahara and X. Xin, *J. Chem. Soc., Dalton Trans.*, 1997, 2357; (*c*) C. Zhang, Y. Song, G. Jin, G. Fang, Y. Wang, S. S. S. Raj, H.-K. Fun and X. Xin, *J. Chem. Soc., Dalton Trans.*, 2000, 1317; (*d*) C. Zhang, Y. Song, Y. Xu, H. Fun, G. Fang, Y. Wang and X. Xin, *J. Chem. Soc., Dalton Trans.*, 2000, 2823.

26 (*a*) S. Shi, H. W. Hou and X. Q. Xin, *J. Phys. Chem.*, 1995, **99**, 4050; (*b*) W. Ji, S. Shi, H. J. Du, P. Ge, S. H. Tang and X. Q. Xin, *J. Phys. Chem.*, 1995, **99**, 17297.

27 W. Ji, H. J. Du, S. H. Tang and S. Shi, *J. Opt. Soc. Am. B*, 1995, **12**, 876; T. Xia, A. Dogariu, K. Mansour, D. J. Hagan, A. A. Said, E. W. Van Stryland and S. Shi, *J. Opt. Soc. Am. B*, 1998, **15**, 1497.